Journal of Hydrospace Technology, Vol. 2, No. 2, 1996, pp. 57-67

Hybrid-QUICK Scheme Using Finite-Volume Method

Jung-Eun Choi*

Abstract

The formulation for hybrid-QUICK scheme of convective transport terms in finite-volume calculation procedure is presented. Source terms are modified to apply the hybrid-QUICK scheme. Test calculations are performed for wall-driven cavity flow at Re = 10^2, 10^3, and 10^4. These include the evaluation of boundary conditions approximated by third-order finite difference scheme. The stable and converged solutions are obtained without unsteady terms in the momentum equations. The results using hybrid-QUICK scheme show no difference with those using hybrid scheme at low Re (=10^2) and are better at higher Re (=10^3 and 10^4).

1 Introduction

Many researches have done to treat the convection terms in the Navier-Stokes (NS) equations to obtain stable solutions at high Reynolds number(Re) and vortical flow; a first-order-accurate upwind differencing[1], a hybrid of first-order upwind and central-differencing[2], a third-order-accurate upwind scheme[3, 4]. Hayase et al.[5] also present formulation for this scheme using a first-order-accurate upwind scheme. Kang et al.[6] compared the results from the various schemes, i.e., 2nd- and 4th-order central and 1st-, 2nd-, 3rd-order upwind scheme. Agawal[3], Hayase et al.[5], and Kang et al.[6] succeed to obtain accurate and stable solutions for a wall-driven cavity flow at high Re (= 10^4). The use of a high resolution upwind scheme in an implicit solution procedure results in nondiagollay dominant matrices and can lead to numerical instabilities. One of techniques to remedy these instabilities is that the matrix remains diagonally dominant throughout iterative procedure. In this paper, the same diagonal matrix formulation of hybrid scheme is retained by changing source terms to apply the QUICK scheme. And the wall-driven cavity flow is calculated by applying the boundary conditions approximated by the third-order finite difference scheme.

2 Computational Method

Computational method is based on extensions of TEACH code (Gosman and Ideriah[7], or Oh[8]), which applies the staggered-grid arrangement for the velocities (Fig. 1) and

*Member,Maritime Research Institute Hyundai Industries Co., Ltd.

SIMPLE algorithm for the coupling of the velocity and pressure field. The continuity and NS equations for incompressible viscous flow are written in the physical domain using two-dimensional Cartesian coordinates (x, y). In the non-dimensional form, the equations are:

$$\frac{\partial U}{\partial x} + \frac{\partial V}{\partial y} = 0 \tag{1}$$

$$\frac{\partial}{\partial x}(U\phi) + \frac{\partial}{\partial y}(V\phi) = \frac{\partial}{\partial x}\left(\Gamma_\phi \frac{\partial \phi}{\partial x}\right) + \frac{\partial}{\partial y}\left(\Gamma_\phi \frac{\partial \phi}{\partial y}\right) + S_\phi \tag{2}$$

where $\phi = (U, V)$, $\Gamma_\phi = \frac{1}{Re}$, $\mathrm{Re} = \frac{U_o L}{\nu}$, and $S_\phi = \left(-\frac{\partial p}{\partial x}, -\frac{\partial p}{\partial y}\right)$

Equations (1) and (2) are transformed into nonorthogonal curvilinear coordinates. A partial transformation is used. Then (2) becomes

$$\left[\frac{\partial}{\partial \xi}(C^\xi \phi) - \frac{\partial}{\partial \xi}\left(D^\xi \frac{\partial \phi}{\partial \xi}\right)\right] + \left[\frac{\partial}{\partial \eta}(C^\eta \phi) - \frac{\partial}{\partial \eta}\left(D^\eta \frac{\partial \phi}{\partial \eta}\right)\right] - S_\phi' = 0 \tag{3}$$

where

$$C^\xi = (b_1^1 U + b_2^1 V), \qquad D^\xi = (\Gamma_\phi J g^{11})$$

$$C^\eta = (b_1^2 U + b_2^2 V), \qquad D^\eta = (\Gamma_\phi J g^{22})$$

$$S_\phi' = \frac{\partial}{\partial \xi}\left(\Gamma_\phi J g^{12} \frac{\partial \phi}{\partial \eta}\right) + \frac{\partial}{\partial \eta}\left(\Gamma_\phi J g^{21} \frac{\partial \phi}{\partial \xi}\right) + J S_\phi$$

Here, b_j^i are geometric coefficients and superscripts (ξ, η) are the plane of control volume. In the hybrid scheme of finite-volume method, integration of ϕ for the control volume gives;

$$\begin{aligned} &\int\int \left[\frac{\partial}{\partial \xi}(C^\xi \phi) - \frac{\partial}{\partial \xi}\left(D^\xi \frac{\partial \phi}{\partial \xi}\right)\right] d\xi\, d\eta \\ &= C^\xi \phi\Big|_d - C^\xi \phi\Big|_u + D^\xi \frac{\partial \phi}{\partial \xi}\Big|_u - D^\xi \frac{\partial \phi}{\partial \xi}\Big|_d \\ &= (a_D + a_U + C_d^\xi - C_u^\xi)\,\phi_P - a_D \phi_D - a_U \phi_U \end{aligned} \tag{4}$$

and

$$\begin{aligned}
&\int\int \left[\frac{\partial}{\partial\eta}(C^\eta\phi) - \frac{\partial}{\partial\eta}\left(D^\eta\frac{\partial\phi}{\partial\eta}\right)\right] d\xi\, d\eta \\
&= C^\eta\phi\Big|_n - C^\eta\phi\Big|_s + D^\eta\frac{\partial\phi}{\partial\eta}\Big|_s - D^\eta\frac{\partial\phi}{\partial\eta}\Big|_n \\
&= (a_N + a_S + C_n^\eta - C_s^\eta)\,\phi_P - a_N\phi_N + a_S\phi_S
\end{aligned} \tag{5}$$

where

$$a_D = [-C_d^\xi, D_d^\xi - C_d^\xi/2, 0]_{\max}$$

$$a_U = [+C_u^\xi, D_u^\xi + C_u^\xi/2, 0]_{\max}$$

$$a_N = [-C_n^\eta, D_n^\eta - C_n^\eta/2, 0]_{\max}$$

$$a_S = [+C_s^\eta, D_s^\eta + C_s^\eta/2, 0]_{\max}$$

$$C_u^\xi = (b_1^1 U + b_2^1 V)_u \qquad D_u^\xi = (\Gamma_\phi J g^{11})_u$$

$$C_d^\xi = (b_1^1 U + b_2^1 V)_d \qquad D_d^\xi = (\Gamma_\phi J g^{11})_d$$

$$C_n^\eta = (b_1^2 U + b_2^2 V)_n \qquad D_n^\eta = (\Gamma_\phi J g^{22})_n$$

$$C_s^\eta = (b_1^2 U + b_2^2 V)_s \qquad D_s^\eta = (\Gamma_\phi J g^{22})_s$$

and

$$\int\int S_\phi'\, d\xi\, d\eta = \overline{S_\phi}' \tag{6}$$

where the subscripts (D,U,N,S,d,u,n,s) and superscript (-) are the nodal points and integration value for the control volume, respectively. Then, the following five-point finite-volume algebraic equation is obtained

$$a_P\phi_P = a_N\phi_N + a_S\phi_S + a_D\phi_D + a_U\phi_U + \overline{S_\phi}' \tag{7}$$

where

$$a_P = a_N + a_S + a_D + a_U + (C_d^\xi - C_u^\xi + C_n^\eta - C_s^\eta) \tag{8}$$

The QUICK scheme employs quadratic interpolation technique using two-point upstream and one-point downstream within the context of a control-volume approach for calculating on a staggered grid (Fig. 1). Then we obtain the velocities at nodes (d,u,n,s) from the above scheme assumption (Table 1). By substituting the velocities of Table 1 into (4) and (5), we can obtain the equations using QUICK scheme. Then,

the differences between these equations and the hybrid equations give the additional source terms due to QUICK scheme ($=\Delta\overline{S_\phi}''$), i.e.,

$$a_P\phi_P = a_D\phi_D + a_U\phi_U + a_N\phi_N + a_S\phi_S + \overline{S_\phi}' + \triangle\overline{S_\phi}'' \tag{9}$$

where $\Delta\overline{S_\phi}'' = \Delta\overline{S_{\xi\phi}}'' + \Delta\overline{S_{\eta\phi}}''$. The values of $\Delta\overline{S_{\xi\phi}}''$ and $\Delta\overline{S_{\eta\phi}}''$ are shown in Table 2.

A third-order formulations which are applied at the boundary are illustrated at Fig. 2. In the case where ϕ is perpendicular to wall and $C_u^\xi > 0$ (Fig. 2a), the velocity at node u is changed, i.e.,

$$\phi_u = -\frac{1}{8}\phi_D + \frac{3}{4}\phi_P + \frac{3}{8}\phi_U = \left(\frac{3}{8}\phi_P + \frac{3}{4}\phi_U - \frac{1}{8}\phi_{UU}\right) - \frac{1}{8}\phi_D + \frac{3}{8}\phi_P - \frac{3}{8}\phi_U + \frac{1}{8}\phi_{UU}$$

Then, the additional source term $(\Delta S_{b\xi\phi}'')$ at the boundary is

$$\triangle\overline{S_{b\xi\phi}}'' = C_u^\xi\left(-\frac{1}{8}\phi_D + \frac{3}{8}\phi_P - \frac{3}{8}\phi_U + \frac{1}{8}\phi_{UU}\right) \tag{10}$$

By the same way, in the case where ϕ is parallel to wall and $C_u^\xi > 0$ (Fig. 2b),

$$\triangle\overline{S_{b\xi\phi}}'' = C_u^\xi\left(-\frac{1}{24}\phi_P + \frac{1}{4}\phi_U - \frac{1}{8}\phi_{UU} + \frac{1}{3}\phi_b\right) \tag{11}$$

where ϕ_b is the velocity at the boundary.

3 Computational Conditions

Numerical calculations are performed for the wall-driven cavity flow. The values of Re to be investigated are 10^2, 10^3, and 10^4. The grids are generated by analytic method. The grid effects are studied from the centerline velocity components at the various grid no. from 31x31 to 81x81 by increasing 10x10. The results of Hybrid scheme, which are not presented in this paper, show that the denser the grid is, the closer is the solution to the Ghia et al.[9]. However, the results of Hybrid-QUIK scheme, show the numerical errors for the denser grid ($\geq$ 61x61), especially at higher Re no.($=10^4$), due to small values of Jacobian and numerical diffusion. Therefore, 51 x 51 grids are adopted (see Fig. 3). Underrelaxation factors for velocities and pressure (= 0.5) are used. The

values of residuals of $\phi(= U, V, p)$ are less than 10^{-4} (Fig. 4), where the residual is defined by

$$Residual(it) =$$

$$\sum_{i=1}^{ni}\sum_{j=1}^{nj} \| \phi(it-1) | - | \phi(it) \| \Big/ \sum_{i=1}^{ni}\sum_{j=1}^{nj} | \phi(itl) | \tag{12}$$

where it, itl, ni, and nj is iteration, last iteration number, grid number in ξ- and η -direction, respectively. The calculations are performed on IBM 9076.

4 Results and Conclusions

Centerline velocity profiles for U and V velocity components are shown in Fig. 5. The U and V plots are along vertical and horizontal lines, respectively. These values are compared with the results of Ghia et al.[9]. At low Re ($= 10^2$), there is no difference between the results of hybrid and hybrid-QUICK scheme. As Re increases, the differences become larger showing that the results using the QUICK scheme are more accurate. However, these are a little different from the results of Ghia et al.[7] at the region of low speed and high velocity gradient. The contours of stream functions and equivorticity lines are shown in Fig. 6 and Fig. 7, respectively. As shown in Fig. 6, the magnitudes and shapes of the contours of hybrid-QUICK scheme are very similar to those of hybrid scheme at low Re ($= 10^2$). As Re increases, the contour shapes and magnitudes of hybrid-QUICK scheme are much different with those of the hybrid scheme. The same tendency can be seen in the equivorticity lines (Fig. 7). Fig. 7 show the development of a central, nearly circular vortex, with bottom (and side) secondary vortices. At Re $= 10^4$, a tertiary vortex in the bottom (and side) appears in hybrid-QUICK scheme, whereas no tertiary vortex in hybrid scheme. The region of the tertiary vortex is a little smaller than those of Ghia et al.[9]. From these results, the more stable and converged solutions can be obtained by using the hybrid-QUICK scheme, especially, at high Re.

References

[1]] Nallasamy, M. and Prasad, K.K., "Numerical Studies on Quasilinear and Linear Elliptic Equations", J. of Computational Physics, Vol. 15, pp. 429-448, 1974.

[2] Patankar, S.V. and Spalding, D.B., "A Calculation Procedure for Heat, Mass and Momentum Transfer in Three-Dimensional Parabolic Flows", Int. J. Heat Mass Transfer, Vol. 15, pp. 1797-1806, 1972.

[3] Agarwal, R.K., "A Third-Order-Accurate Upwind Scheme for Navier-Stokes Solutions at High Reynolds Numbers", AIAA Paper, No. 81-0112, 1981.

[4] Leonard, B.P., "A Stable and Accurate Convective Modelling Procedure Based on Quadratic Upstream Interpolation", Computer Methods in Applied Mechanics and Engineering, Vol. 19, pp. 59-98, 1979.

[5] Hayase, T., Humphery, J.A.C., and Greif, R., "A Consistently Formulated QUICK Scheme for Fast and Stable Convergence Using Finite-Volume Iterative Calculation Procedures", J. of Computational Physics, Vol. 98, pp. 108-118, 1992.

[6] Kang, K.J., Park, Y.J., and Jo, K,J, "Study on the Differencing Scheme for Convection Terms of the 2-Dimensional Navier-Stokes Equations", The Spring Meeting of SNAK., pp. 148-155, 1991.

[7] Gosman, A.D. and Ideriah, F.J.K, TEACH-2E Computation Code Manual, Dep't of Mechanical Engineering, Imperial College, London, 1976.

[8] Oh, K.J., "Numerical Study on Viscous Flows around the Ship Stern", Ph.D. Thesis, Seoul National University, Korea, 1989.

[9] Ghia, U., Ghia, K.N., and Shin, C.T., "High-Re Solutions for incompressible Flow Using the Navier-Stokes Equations and a Multi-Grid Methods", J. of Computational Physics, Vol. 48, pp. 387-411, 1982.

Table 1: Velocities at nodes d, u, n, and s

C_d^ξ	ϕ_a	C_u^ξ	ϕ_u
+	$\frac{3}{8}\phi_D+\frac{3}{4}\phi_P-\frac{1}{8}\phi_U$	+	$\frac{3}{8}\phi_P+\frac{3}{4}\phi_U-\frac{1}{8}\phi_{UU}$
-	$-\frac{1}{8}\phi_{DD}+\frac{3}{4}\phi_D+\frac{3}{8}\phi_F$	-	$-\frac{1}{8}\phi_D+\frac{3}{4}\phi_P+\frac{3}{8}\phi_U$
C_n^η	ϕ_n	C_s^η	ϕ_s
+	$\frac{3}{8}\phi_N+\frac{3}{4}\phi_P-\frac{1}{8}\phi_S$	+	$\frac{3}{8}\phi_P+\frac{3}{4}\phi_S-\frac{1}{8}\phi_{SS}$
-	$-\frac{1}{8}\phi_{NN}+\frac{3}{4}\phi_N+\frac{3}{8}\phi_F$	-	$-\frac{1}{8}\phi_N+\frac{3}{4}\phi_P+\frac{3}{8}\phi_S$

Table 2: Additional source terms in QUICK scheme

C_a^ξ	C_u^ξ	$\triangle \overline{S_{\xi\phi}}''$
+	+	$\left(a_D+a_U+\frac{1}{4}C_d^\xi-\frac{5}{8}C_u^\xi-D_d^\xi-D_u^\xi\right)\phi_P+\left(D_d^\xi-\frac{3}{8}C_d^\xi-a_D\right)\phi_D$ $+\left(D_u+\frac{1}{8}C_d^\xi+\frac{3}{4}C_u^\xi-a_U\right)\phi_U-\frac{1}{8}C_u^\xi\phi_{UU}$
+	-	$\left(a_D+a_U+\frac{1}{4}C_d^\xi-\frac{1}{4}C_u^\xi-D_u^\xi-D_d^\xi\right)\phi_P$ $+\left(D_d^\xi-\frac{3}{8}C_d^\xi-\frac{1}{8}C_u^\xi-a_D\right)\phi_D+\left(D_u^\xi+\frac{1}{8}C_d^{\xi+}\frac{3}{8}C_u^\xi-a_U\right)\phi_U$
-	+	$\left(a_D+a_U+\frac{5}{8}C_d^\xi-\frac{5}{8}C_u^\xi-D_u^\xi-D_d^\xi\right)\phi_P+\left(D_d^\xi-\frac{3}{4}C_d^\xi-a_D\right)\phi_D$ $+\left(D_u^\xi+\frac{3}{4}C_u^\xi-a_U\right)\phi_U+\frac{1}{8}C_d^\xi\phi_{DD}-\frac{1}{8}C_u^\xi\phi_{UU}$
-	-	$\left(a_D+a_U+\frac{5}{8}C_d^\xi-\frac{1}{4}C_u^\xi-D_d^\xi-D_u^\xi\right)\phi_P$ $+\left(D_d^\xi-\frac{3}{4}C_d^\xi-\frac{1}{8}C_u^\xi-a_D\right)\phi_D+\left(D_u^\xi+\frac{3}{8}C_u^\xi-a_U\right)\phi_U+\frac{1}{8}C_d^\xi\phi_{DD}$

C_n^η	C_s^η	$\triangle \overline{S_{\eta\phi}}''$
+	+	$\left(a_N+a_S+\frac{1}{4}C_n^\eta-\frac{5}{8}C_s^\eta-D_n^\eta-D_s^\eta\right)\phi_P+\left(D_n^\eta-\frac{3}{8}C_n^\eta-a_N\right)\phi_N$ $+\left(D_s+\frac{1}{8}C_n^\eta+\frac{3}{4}C_s^\eta-a_S\right)\phi_S-\frac{1}{8}C_s^\eta\phi_{SS}$
+	-	$\left(a_N+a_S+\frac{1}{4}C_n^\eta-\frac{1}{4}C_s^\eta-D_s^\eta-D_n^\eta\right)\phi_P$ $+\left(D_n^\eta-\frac{3}{8}C_n^\eta-\frac{1}{8}C_s^\eta-a_N\right)\phi_N+\left(D_s^\eta+\frac{1}{8}C_n^\eta+\frac{3}{8}C_s^\eta-a_S\right)\phi_S$
-	+	$\left(a_N+a_S+\frac{5}{8}C_n^\eta-\frac{5}{8}C_s^\eta-D_s^\eta-D_n^\eta\right)\phi_P+\left(D_n^\eta-\frac{3}{4}C_n^\eta-a_N\right)\phi_N$ $+\left(D_s^\eta+\frac{3}{4}C_s^\eta-a_S\right)\phi_S+\frac{1}{8}C_n^\eta\phi_{NN}-\frac{1}{8}C_s^\eta\phi_{SS}$
-	-	$\left(a_N+a_S+\frac{5}{8}C_n^\eta-\frac{1}{4}C_s^\eta-D_n^\eta-D_s^\eta\right)\phi_P$ $+\left(D_n^\eta-\frac{3}{4}C_n^\eta-\frac{1}{8}C_s^\eta-a_N\right)\phi_N+\left(D_s^\eta+\frac{3}{8}C_s^\eta-a_S\right)\phi_S+\frac{1}{8}C_n^\eta\phi_{NN}$

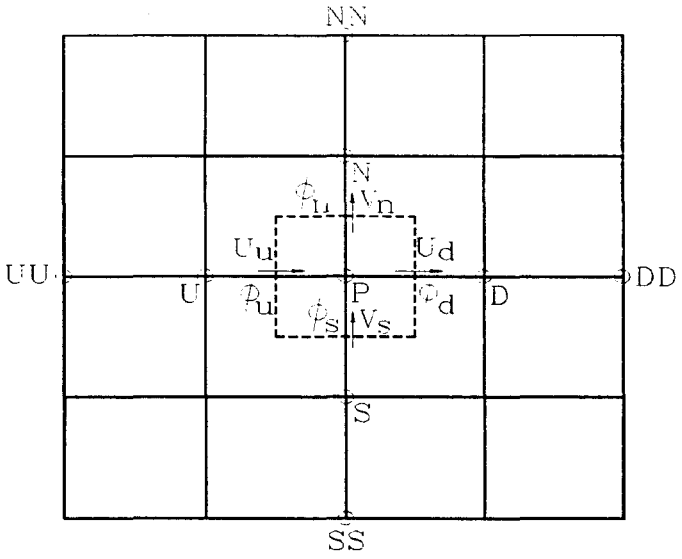

Figure 1: Staggered grid

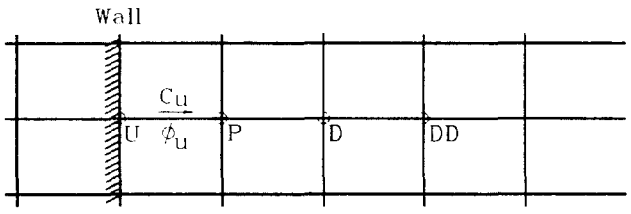

(a) ϕ is perpendicular to the wall

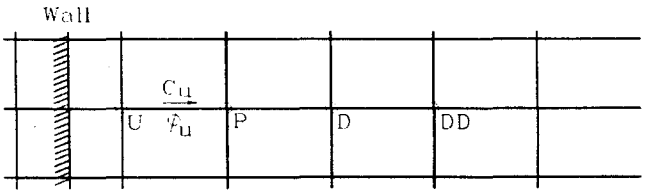

(b) ϕ is parallel to the wall

Figure 2: Third-order representations of near boundary

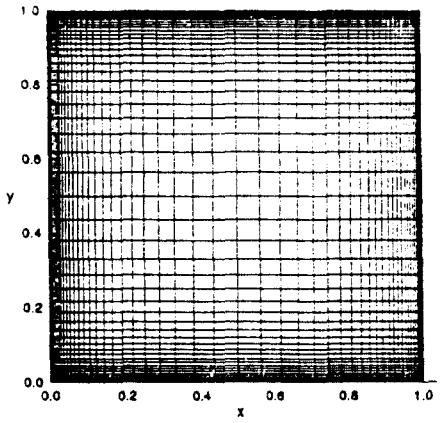

Figure 3: Computational grids and coordinate systems

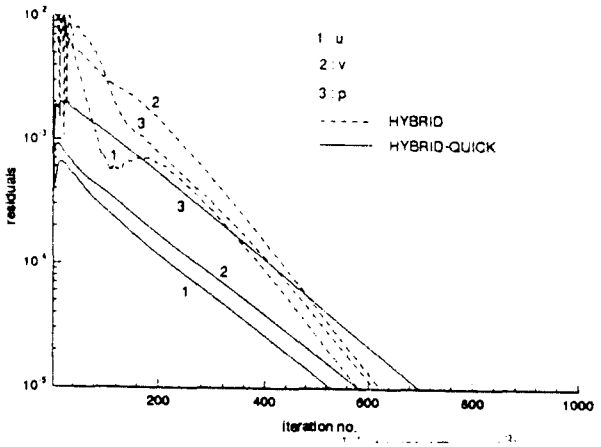

Figure 4: Convergence history ($Re=10^3$)

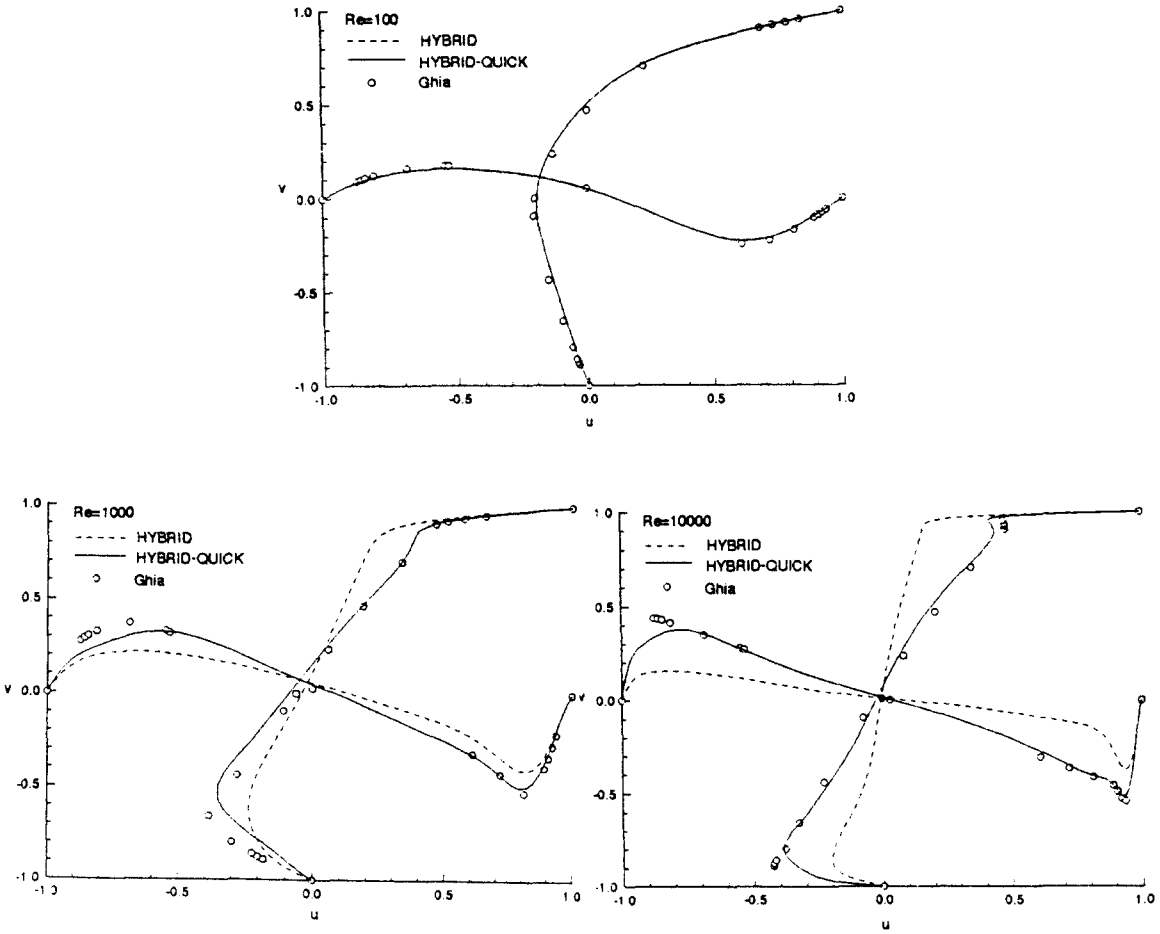

Figure 5: Centerline velocity components

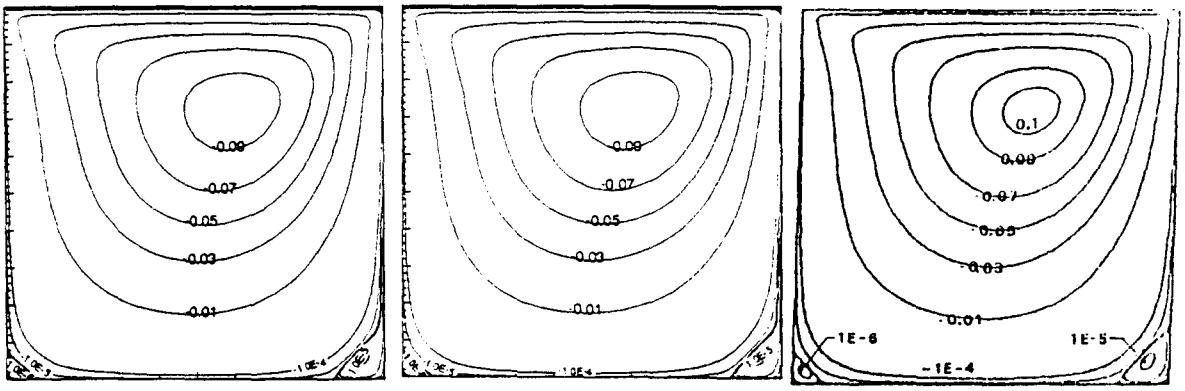

(a) hybrid, Re = 10^2 (b) QUICK, Re = 10^2 (c) Ghia, Re = 10^2

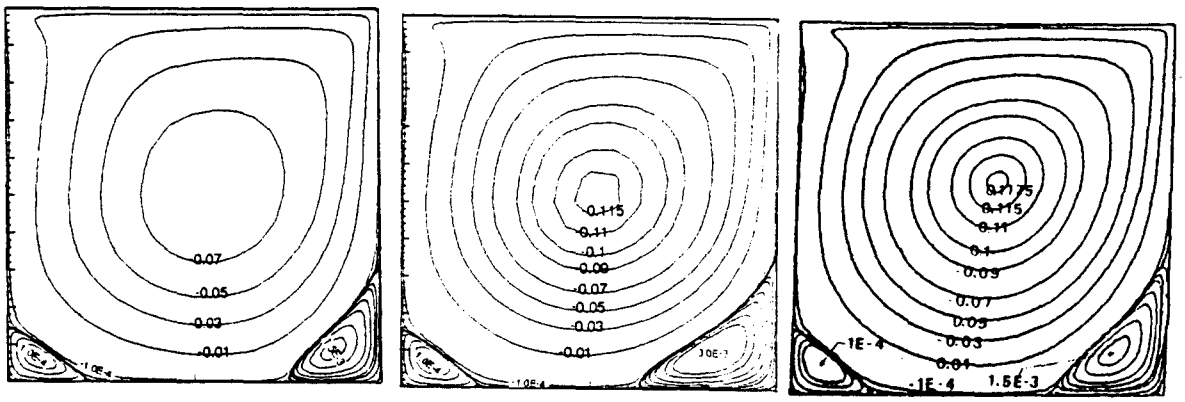

(d) hybrid, Re = 10^3 (e) QUICK, Re = 10^3 (f) Ghia, Re = 10^3

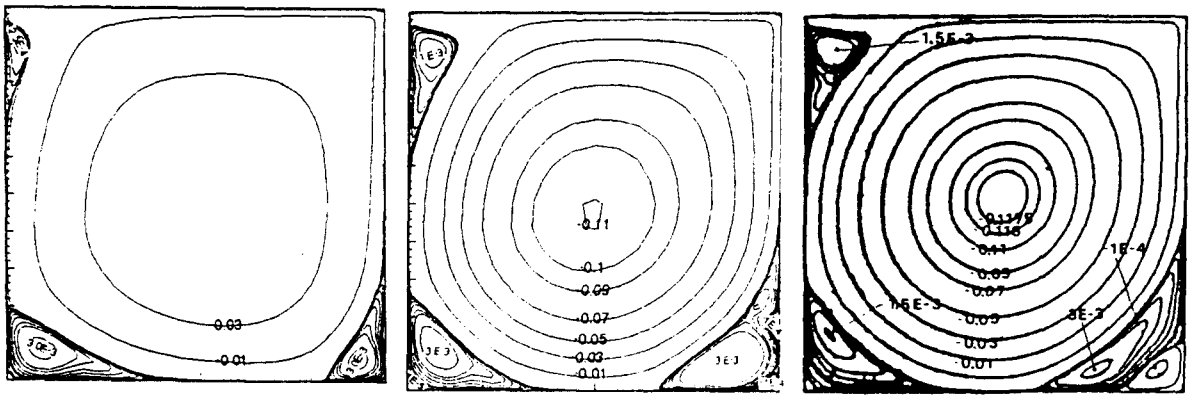

(g) hybrid, Re = 10^4 (h) QUICK, Re = 10^4 (i) Ghia, Re = 10^4

Figure 6: Stream functions

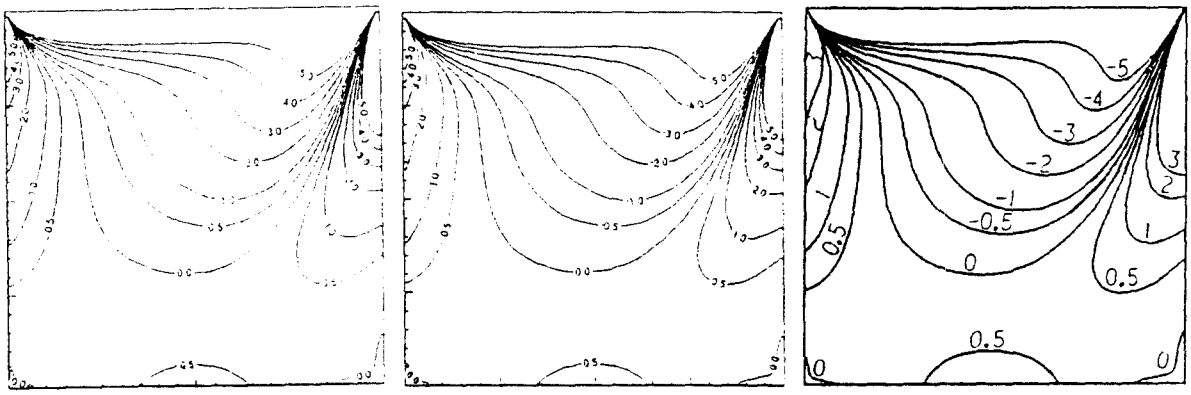

(a) hybrid, Re = 10^2 (b) QUICK, Re = 10^2 (c) Ghia, Re = 10^2

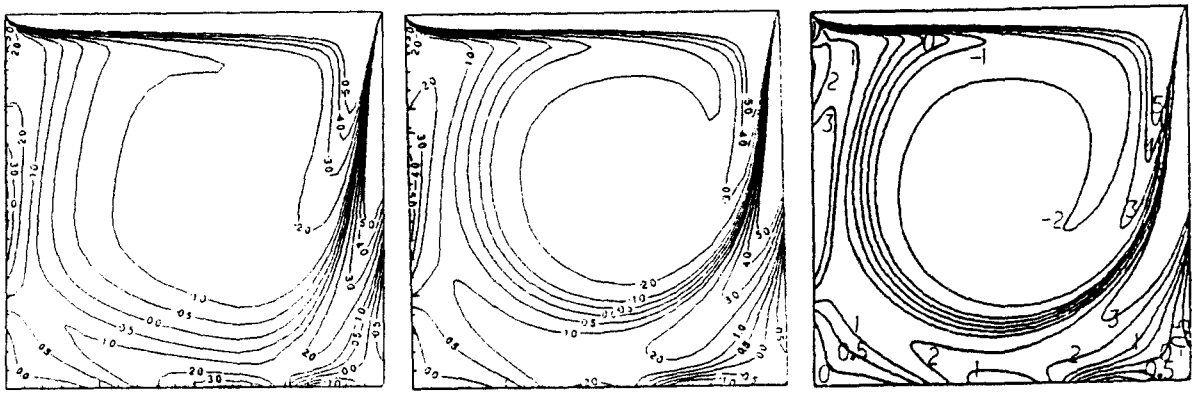

(d) hybrid, Re = 10^3 (e) QUICK, Re = 10^3 (f) Ghia, Re = 10^3

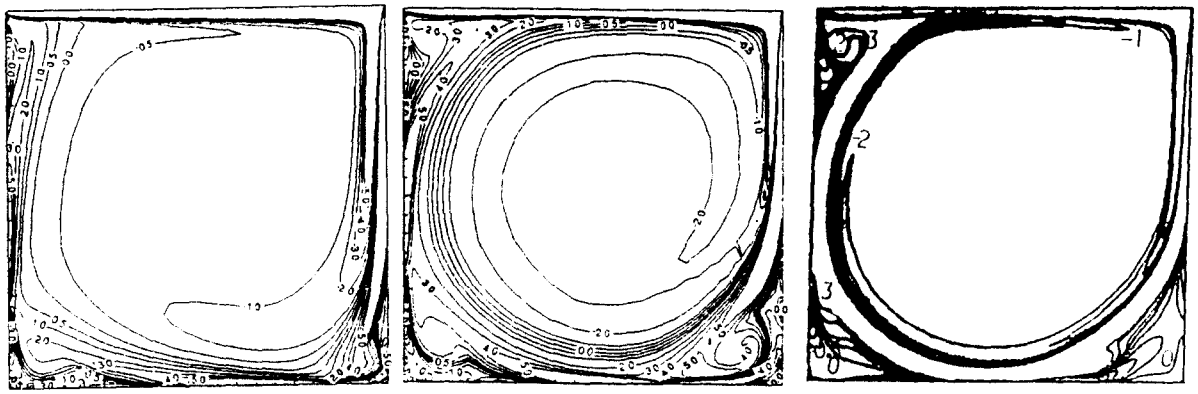

(g) hybrid, Re = 10^4 (h) QUICK, Re = 10^4 (i) Ghia, Re = 10^4

Figure 7: Equivorticity lines